Self-Assembly and Optical Behavior of Mangetic-Plasmonic Nanostructures

Kai Liu[1], Xiaozheng Xue[2], Viktor Sukhotskiy[1] and Edward P. Furlani[1,2,*]

[1]Dept. of Electrical Engineering, University at Buffalo SUNY, NY 14260
[2]Dept. of Chemical and Biological Engineering, University at Buffalo SUNY, NY 14260
[*]efurlani@buffalo.edu

ABSTRACT

We present a bottom-up method for the fabrication of nanostructured photonic media and demonstrate proof-of-principle using a multiphysics modeling approach. The method involves magnetic field-directed template-assidted self-assembly of magnetic-plasmonic core-shell particles (e.g. Fe_3O_4@Au) into extended particle superstructures that have a desired photonic functionality. The superparamagnetic core enables adaptive magnetophoretic control of particle motion and provides interparticle coupling that drives the assembly process. The plasmonic shell provides unique optical and photothermal properties of assembled structures. Monte Carlo analysis and full-wave field theory are combined to investigate self-assembly and optical properties of particle superstructures. We demonstrate the method for two different Fe_3O4@Au particle assemblies: heptamer particle structures and 1D particle chains. We demonstraet that the former supports Fano resonance behavior, while the latter exhibits extraordinary field enhancement and focused photothermal transduction.

.

Keywords: Localized surface plasmon resonance (LSPR), plasmonic nanocages, photothermal energy conversion, LSPR-induced optical absorption, pulsed-laser photothermal heating, photothermal therapy.

1 HEPATMER STRUCTURES: FANO RESONANCE

We use 3D full-wave field analysis to study the optical behaviour of a self-asembled heptamer structure that consists of seven Fe_3O_4@Au core-shell nanoparticles as shown in **Figure 1**. **Figure 1a** illustrates the geometry of an individual core-shell particle that consists of a Fe_3O_4 core with a radius R_c and a gold shell with a thickness t_s. The Fe_3O_4@Au nanoparticles can be magentized and manipulated using an external magnetic field and they exhibit a plasmonic spectral response that can be tuned by adjusting the thickness of the metalic shell. **Figure 1b** shows the computational domain (CD) for the field analysis, which was performed using the finite element based RF module from Comsol (www.comsol.com). In the CD, seven core-shell particles are closely packed on a glass substrate (SiO_2) with a uniform end-to-end spacing distance S and immersed in water (H_2O). The cluster is illuminated with a downward-directed plane wave with the **E** field polarized along the x-axis [1]. This analyis shows that the heptamer structure exhibits Fano resonance features that depend on geometric parameters as well as the surrounding medium.

1.1 Self-Assembly of Heptamer Structures

The heptamer particle structures are self-assembled using a magnetic template in the form of a nanostructured cylindrical permanent magnet. The self- assembly of a 4 x 4 array of such structures is illustrated in **Fig. 2**. It is instructive to inestigate the dominant magnetic field that the templates provide. i.e. the z-component B_z at different vertical distances, S_v = 50 nm, 100 nm and 150 nm, from the top surface of the template. This data is plotted in **Fig. 2a-2c** and reveals the vertical gradient of the magnet field and its strong localization in proximity of the top surface of the magnets. This imples that the particles in proximity to a template will assemble on it, rayher than drift to a neihboring magnet. Next, we use the Monte Carlo method with the Metropolis algorithm to determine the self-assembled equilibrium structure of monodisperse Fe_3O_4@Au core-shell particles with dimensions of R_c = 25 nm and t_s = 12 nm. This analysis takes into account several competitive effects including induced magnetic dipole-dipole interactions, the electrostatic interparticle repulsion based on DLVO theory, Brownian dynamics, Van der Waals interaction, hydrodynamic interactions and a steric

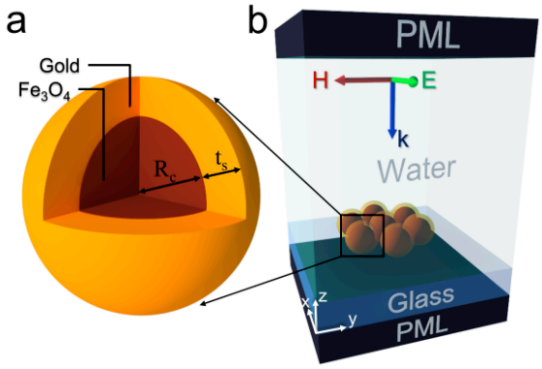

Figure 1. Magnetic-plasmonic nanostructures and the computational model (CD): (a) Fe_3O_4@Au core-shell particle, (b) CD showing the polarization and propagation direction of the incident field.

TechConnect Briefs 2017, TechConnect.org, ISBN 978-0-9988782-1-8

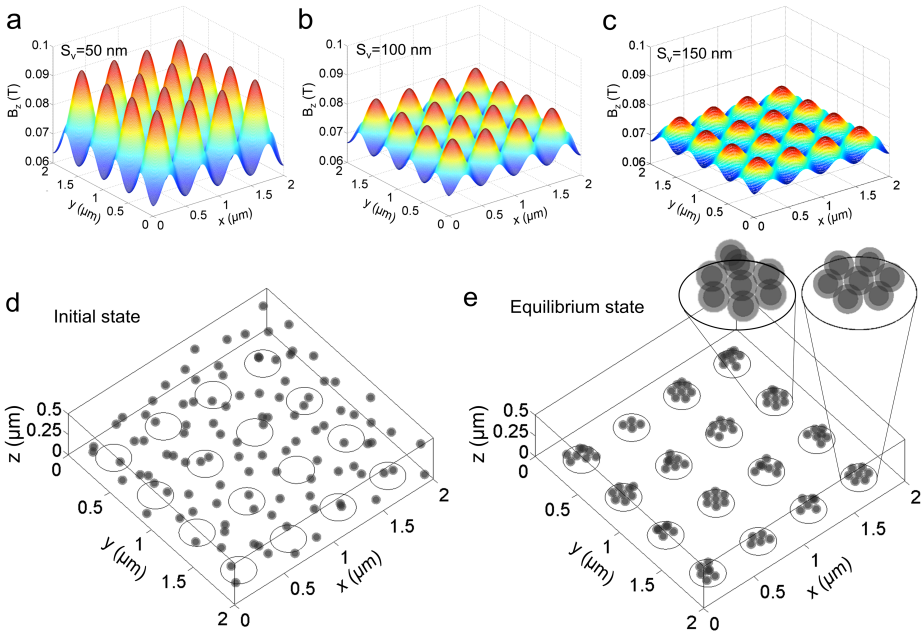

Figure 2. Self-assembly of the heptamer particle structure using a template-assisted protocol based on an array of 4×4 nanostructured cylindrical permanent magnets: (a)-(c) Magnetic flux B_z of the 4×4 array at distances of S_v=50, 100, and 150 nm above the template. (d)-(e) Self-assembly of the heptamer at (d) the initial state and (e) the final equilibrium state. The insets are examples of the perfect heptamer and the heptamer with small defects in particle placement. The monodisperse core-shell particle has the dimensions of R_c=25 nm and t_s=12 nm.

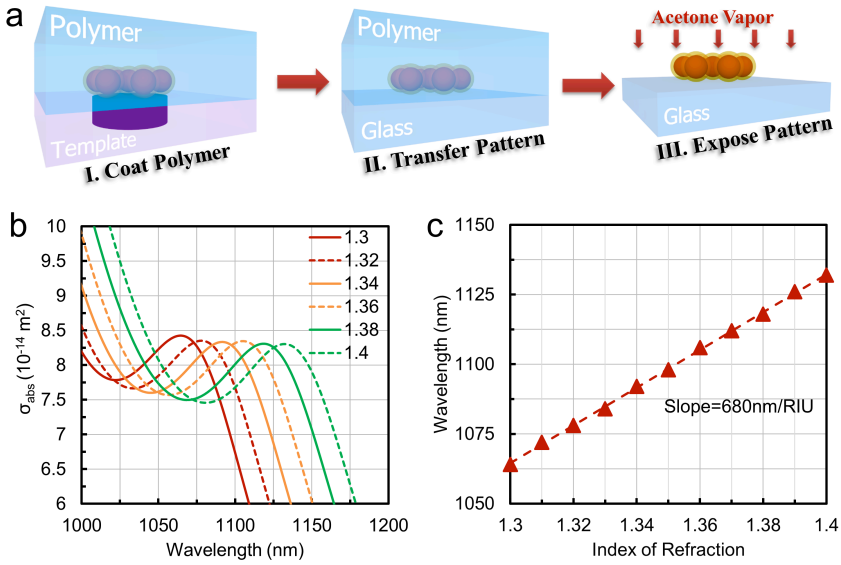

Figure 3. Biosensing applications of the magnetic-plasmonic heptamer: (a) The protocol of the pattern transfer: I. Immerse the heptamer array in a polymeric film; II. Transfer the polymeric film with heptamers onto the glass substrate; III. Remove polymers and expose the polymer to acetone vapor. (b) Fano absorption peak as a function of the refractive index of the environment. (c) The extracted peak wavelengths vs. the surrounding refractive indices.

repulsive force caused by surfactant-surfactant contact. In our analysis, the height of the computational domain is 500 nm and the carrier fluid is water. **Figure 2d-2e** illustrate the self-assembly process. In the initial state (**Figure 2d**), the nanoparticles are randomly distributed within the CD. In the final equilibrium state, the particles have self-assembled over the magnets. For 2 of the 16 magnets (12.5% of the templates), the particles assemble into defect-free heptamer structures. For an additional 3 of the 16 magnets (19% of the templates, **Figure 2e**) the particles assemble into heptamer structures with insignificant defects in particle placement, i.e. the structures exhibit hot spots and Fano a resonance in the absorption spectrum. Thus, in total, 31% of the assembled structures produce the desired optical

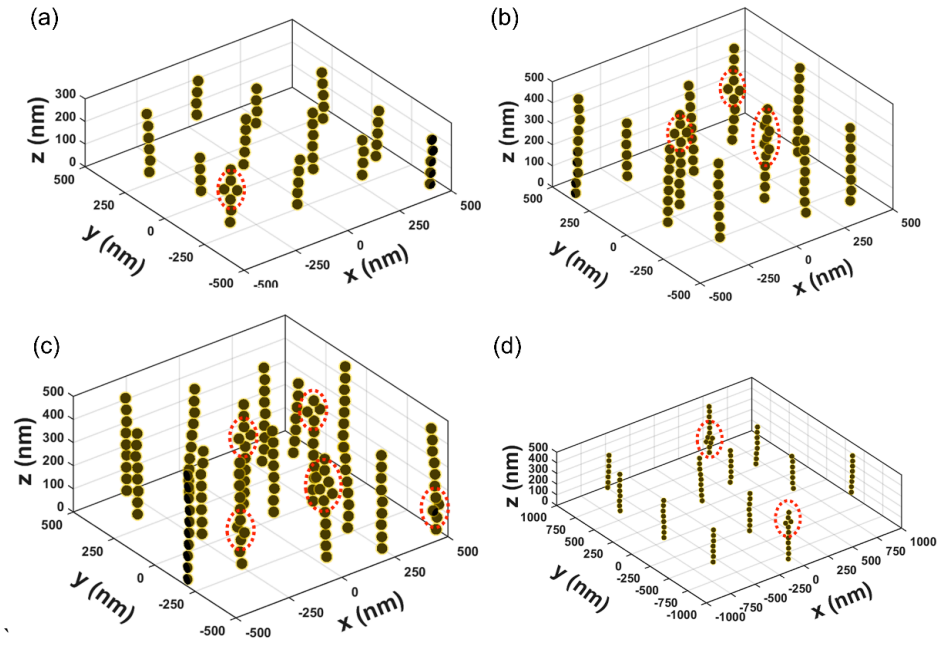

Figure 4. Fe_3O_4@Au chain formation in a nanochannel in the presence of a uniform field with Q=1×10^{-18} C: (a) ϕ = 1.31%, H_c = 300 nm; (b) ϕ = 1.31%, H_c = 500 nm; (c) ϕ = 1.96%, H_c = 300 nm; (d) ϕ = 0.33%, H_c = 500 nm.

response. This can be improved using more complex templates, a focus of our ongoing research.

1.2 Fano Resonance-Biosensing Applications

Once the heptamer structures are assembled, they need to be transfered from the templates to a substrate. We propose a process to transfer the structures to a glass substrate as described in the caption of **Fig. 3a**. The heptamer structures exhibit a Fano resonance. i.e. a local peak in the absorption spectrum as showin in **Fig. 3b.** The Fano resonce is especially sensitve to dimenional parameters as welll as the background media. A key application of a Fano resonance is refractometric biosensing. We use our computational model to study this phenomenon by varying the surrounding refractive index within the range of 1.3-1.4. In doing so, we find a strong dependence of the Fano resonance peak on the background medium. As the refractive index increases, the Fano resonant peak redshifts, as shown in **Figure 3b**. We extract the wavelength of the Fano absorption peak and plot the trend in **Figure 3c**. The results shows a wavelength shift of the absorption peak from 1064 nm to 1132 nm which corresponds to a sensitivity of 680 nm/RIU. We found the sensitivity in our work is comparable with the value, i.e. 674 nm/RIU, reported in the literature, which is based on scattering analysis. [2] The high sensitivity of the Fano resonance absorption peak in the heptamer justifies its strong potential for biosensing applications.

2 ASSEMBLED PARTICLE CHAINS

We now consider the self-assembly of 1D chains of Fe_3O_4@Au particles. We choose a total particle diameter of D_p=50 nm, a Fe_3O_4 core radius of R_c=20 nm and an Au shell thickness of t_s=4 nm, as shown in **Figure 1a**. The particles have a stabilizing surface charge Q and a uniform ultrathin 1 nm coating of surfactant.

2.1 Field-directed Chain Assembly

The self-assembly of particle chains is analyzed using the Monte Carlo method with the Metropolis algorithm [3-4]. If an unbounded colloid is subjected to a uniform field, the particles will self-assemble into long chains of varying length. In oder to contriol the chain length (~10 particles or less) we use a computational domain (CD) that mimics particle confinement in a nanochannel, i.e. the channel is less that 10 particles in height. The parametric analysis for Q = 1×10^{-18} C is shown in **Fig. 4.** In this case, the electrostatic repulsion between the particles is too weak to prevent the formation of zip-chain structures, which are highlighted by red-dashed circles. This is consistent with the energy analysis above and is more prevalent in **Fig. 4c** due to the high volume fraction.

2.2 Photonic Analysis

We investigate the opitcal response of the particle chains using the computational domain shown in **Fig. 5a**. A single chain is centered at the origin of the domain and immersed in H_2O. The particle is illuminated with a uniform downward-directed plane wave with the E field polarized along the chain length, i.e. x-axis. A surface current boundary condition is employed as the excitation source. We predict the absorption spectrum of a 1D particle chain as a function the number of particles N. The chain length ranges from N = 1 to 12 particles and an infinite chain is also considered. The absorption spectra cross section for the different lengths (N) are compared with that of an infinite chain in **Fig. 5b**. The results show that the

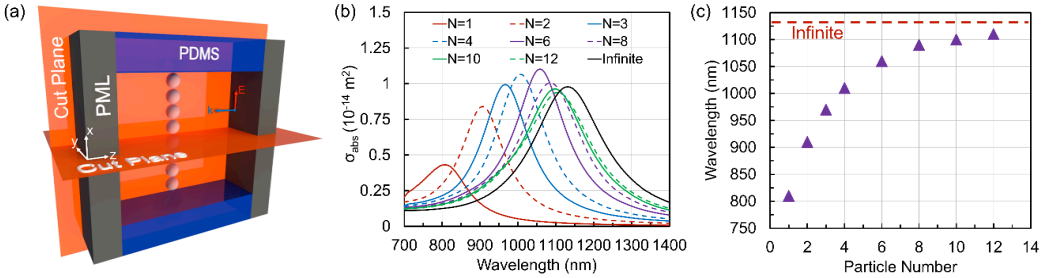

Figure 5. Photonic analysis of 1D particle chains**:** (a) computational domain for photonic analysis; (b) absorption cross section σ_{abs} spectra vs. number (N) of particles in a chain and for an infinite chain (solid black line); (c) LSPR wavelength of 1D chains vs. N. The LSPR wavelength of an infinite chain is indicated by the dashed line.

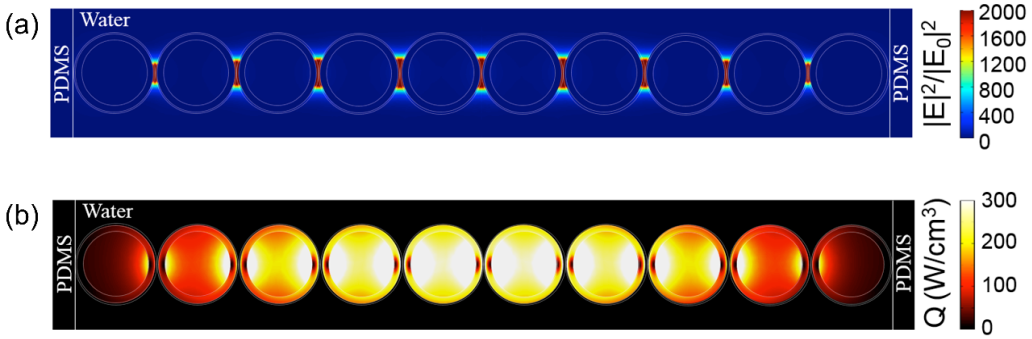

Figure 6. Field enhancement and photothermal transduction**:** (a) local enhancement $|E|^2/|E_0|^2$ and (b) thermal power density in a 1D chain of 10 polymer-coated Fe_3O_4@Au nanoparticles.

absorption spectrum strongly red-shifts from that of a single particle (N =1) and initially grows in amplitude as N increases to 6. As N increase further, the peak absorption decreases slightly and asymptotically approaches that of an infinite chain as the number of particles approaches ~10 (10 to 1 aspect ratio). This is intuitive and clearly seen in **Fig. 5c**, where the LSPR wavelength (triangular markers) of a finite chain rapidly approaches that of an infinite chain (dashed line). This is consistent with previous LSPR studies of chains of solid plasmonic particles [5-6], however our results for Fe_3O_4@Au particle chains is new.

2.3 Photothermal Analysis

Figure 6a shows the spatial profile of the local field enhancement for a 10-particle chain. Each particle has an ultrathin 1 nm thick coating of surfactant. Thus, a nanogap exists between adjacent nanoparticles and the analysis shows that the electric field is strongly concentrated in this deep-subwavelength volume. Then, we investigate the steady-state photothermal energy transduction for the 10-particle chain. Specifically, we compute the steady-state power density generated within the chain due to the conversion of photonic to thermal energy. **Figure 6b** shows the spatial profile of the local thermal energy generation. The strongest heating occurs throughout the center of the chain. This is due to a reduction in the depolarization field (along the length of the chain) in the central particles, which occurs because charges of opposite polarity are induced on the opposing surfaces of neighboring particles on either side of the gap between them. These paired charges of opposite polarity are balanced near the center of the chain due to symmetry (resulting in a substantial reduction of the depolarization field), and become progressively less balanced for particles farther from the center.

REFERENCES

[1] K. Liu, X. Xue, V. Sukhotskiy, E. P. Furlani, J. Phys. Chem. C 120, 27555 (2016).

[2] J. Fan, K. Bao, C. Wu, J. Bao, R. Bardhan, N. J. Halas, V. N. Manoharan, G. Shvets, P. Nordlander, F. Capasso, Nano Lett. 10, 4680 (2010).

[3] X. Xue, J. Wang, E. P. Furlani, ACS Appl. Mater. Interfaces 7, 22515 (2015).

[4] X. Xue, Field-Directed Transport and Self-Assembly of Magnetic Nanoparticles with Applications. Dissertation, University at Buffalo SUNY 2016.

[5] T. H. Chen, M. Pourmand, A. Feizpour, B. Cushman, B. M. Reinhard, J Phys. Chem. C 4, 2147 (2013).

[6] Q. H. Wei, K. H. Su, S. Durant, X. Zhang, Nano Lett. 4, 1067 (2004).